Mass Transfer with Chemical Reaction in a Three-Phase Foam-Slurry Reactor

Studies on mass transfer coupled with chemical reaction were conducted in a gas-liquid-solid foam bed contactor under a variety of operating conditions in order to establish the controlling parameters for such a contacting system. Analytical equations were derived in order to predict the influence of solids dissolution on the specific rate of absorption in the stable foam stage of a three-phase foam-slurry reactor. Experimental investigations on the absorption of carbon dioxide in the presence of an aqueous foam-slurry containing calcium hydroxide particles were carried out in order to verify the theoretical model. Results indicate that the gas-liquid interfacial area and gas flow rate strongly affected the rate of mass transfer, while solids holdup affected mass transfer rates only moderately over the range of solids holdup studied. A comparison with conventional chemical reactor configurations (e.g., bubble column, CSTR) was made to demonstrate the gas-liquid-solid system, for which this novel reactor might be employed. Foam stability enhancement, due to the presence of solid particles, was not observed.

Gregory C. Stangle
R. Mahalingam
Department of Chemical Engineering
Washington State University
Pullman, WA 99164

Introduction

Conventional gas-liquid and gas-liquid-solid reactors and contactors have been studied extensively (Shah, 1978; Froment and Bischoff, 1979; and Ramachandran and Chaudhari, 1983) and well characterized. It would seem that nearly optimal performance of present-day two- and three-phase reactors has been achieved in many cases. It also would seem that significant improvements will not be realized through improvements on the design of existing reactor types, but rather through the development of novel reactor configurations, for example, in bioprocessing. This is especially true in recent years, as energy costs and pollution control have become the focus of much attention in the field of reactor engineering.

The present novel chemical reactor configuration offers a promising alternative to gas-liquid-solid reactor design. Previous work in this laboratory (Shah and Mahalingam, 1984) and elsewhere (Kumar et al., 1981–1987) has focused on mass transfer with chemical reaction in gas-liquid foam. Each investigation has shown that a foam bed contactor provides a relatively large gas-liquid interfacial area and long contact times: both are advantageous in obtaining mass transfer enhancement. On the other hand, each investigation has demonstrated experimentally that foam stability limits gas flow rates through a foam bed reactor (Mahalingam et al., 1975; Mahalingam and Brink, 1978; Surati, 1975; Limaye, 1976), thereby restricting the range of operating conditions. Ralston (1983), however, has described the fact that the presence of small solid particles in foam can lead to foam stability enhancement. If the small solid particles also dissolve into the liquid phase, a chemical reactant can be provided to the liquid phase. The presence of soluble small solid particles in a foam bed reactor should then lead to two significant improvements over two-phase, gas-liquid foam reactors:

1. Since solids dissolution provides a chemical reactant to the aqueous phase, solute mass transfer should be enhanced.
2. Since solid particles might be expected to increase foam stability, a wider range of operating conditions may be achieved.

Hence, the objective of this research was to quantitatively study the influence of sparingly soluble solid particles on gas absorption in a stable three-phase foam-slurry reactor.

Correspondence concerning this paper should be addressed to R. Mahalingam.
Present address of G. C. Stangle: Department of Materials Science and Engineering and the Advanced Materials Technology Program, Washington Technology Center, University of Washington, FB-10, Seattle, WA 98195.

Background

Metzner and Brown (1956) studied CO_2 absorption in a continuous countercurrent foam bed contactor. Mass transfer rates were shown to be 25 to 80 times as high as in packed columns with similar liquid flow rate. Maminov and Mutriskov (1969) studied the absorption of CO_2 in aqueous solutions of NaOH in a foam layer. Their theoretical analysis was based upon the Higbie model, and described a mass transfer coefficient in terms of diffusivity, foam velocity, gas bubble radius, height of foam layer, and gas- and liquid-phase viscosities. Brander et al. (1983) demonstrated the use of aqueous foams for removal of gaseous pollutants from air, showing that hydrogen sulfide, formaldehyde, and acetaldehyde can effectively be absorbed in foam in the presence of chemical reaction with Na_2S, $CuSO_4$, etc. Biswas and Kumar (1981) developed a realistic model, based on the dodecahedral structure of foam, in order to predict absorption rates in a foam bed contactor, where mass transfer occurs in the presence of chemical reaction. Lutsko (1981) developed a mathematical model for the degree of absorption with nonlinear solubility of the gas-phase solute in the presence of an irreversible chemical reaction in a foam layer. Pasiuk-Bronikowska and Sokolowski (1983) studied the oxidation of sodium sulfide to sodium thiosulfate in a semibatch foam bed reactor using air as the oxidizing medium. Shah and Mahalingam (1984) performed theoretical and experimental investigations of CO_2 absorption in sodium hydroxide and in sodium carbonate-sodium bicarbonate solutions in a foam reactor. A theoretical approach based on Danckwerts surface renewal theory was used to interpret experimental results and to evaluate appropriate mass transfer parameters. Bhaskarwar et al. (1987) studied mass transfer with chemical reaction in a foamable liquid-liquid emulsion.

Most published work on foam reactors to date seems to consider only two-phase reaction systems in foam reactors. The presence of small solid particles might be expected to enhance foam stability (Ralston, 1983), since the attainment of the equilibrium gas-liquid-solid contact angle results in the loss of the driving force for further film thinning. If solid particles could be incorporated into a foam reactor, two advantages may result:

- A wider range of operating conditions may be achieved, since solid particles could increase foam stability.
- An entire class of commercially significant processes involving three-phase chemical reaction systems (see, e.g., Shah, 1978; Ramachandran and Chaudhari, 1983) may be improved by exploiting the advantages of a foam slurry reactor.

This concept was first investigated by Stangle (1985), employing the $CO_2/Ca(OH)_2$ system in a foam slurry reactor. Bhaskawar and Kumar (1986) studied a gas-liquid-solid reaction system, in which the solid phase serves as a catalytic site for a gas-liquid reaction, while in the present work the solid phase provides a reactant to the liquid phase to enhance absorption. Very recently, Asolekar et al. (1988) applied the model of Biswas and Kumar (1981) to the system described by Stangle (1985).

The present work is a combined theoretical and experimental effort to evaluate appropriate mass transfer parameters in the latter class of three-phase reactions and to compare the properties of this three-phase foam-slurry reactor configuration with more conventional reactor configurations in order to demonstrate the advantages to be derived.

Model Development

Mass transfer with chemical reaction takes place in a three-phase foam slurry reactor in each of the following stages: the foam formation stage, the stable foam stage, and the foam disengagement stage (see Figure 1).

The process

In the foam formation stage, the gas mixture composed of solute and carrier gases is bubbled through a shallow liquid pool containing surfactant and small solid particles. The surfactant is present in sufficient concentration so as to produce a stable three-phase foam. The pool containing surfactant and slurry is supported by a perforated plate (e.g., wire mesh screen, sieve plate, and fritted glass disc). After foam formation, the gas bubbles separated by thin liquid walls enter the stable foam stage. This foam flows upward under a pressure gradient, until it reaches the foam disengagement stage. After having traveled a predetermined distance in the stable foam stage, the foam is destroyed by chemical or mechanical means.

Mass transfer with chemical reaction takes place in all three stages. The time for foam breakup in the disengagement section is quite short, hence gas absorption during this step may be considered negligible. Mass transfer during foam formation has been estimated and is discussed elsewhere (Stangle, 1985; Stangle and Mahalingam, 1989). The present work evaluates the phenomenon of mass transfer with chemical reaction during the stable foam stage only.

Gas absorption rate

As discussed in the experimental section following, the chemical reaction system under experimental investigation was the

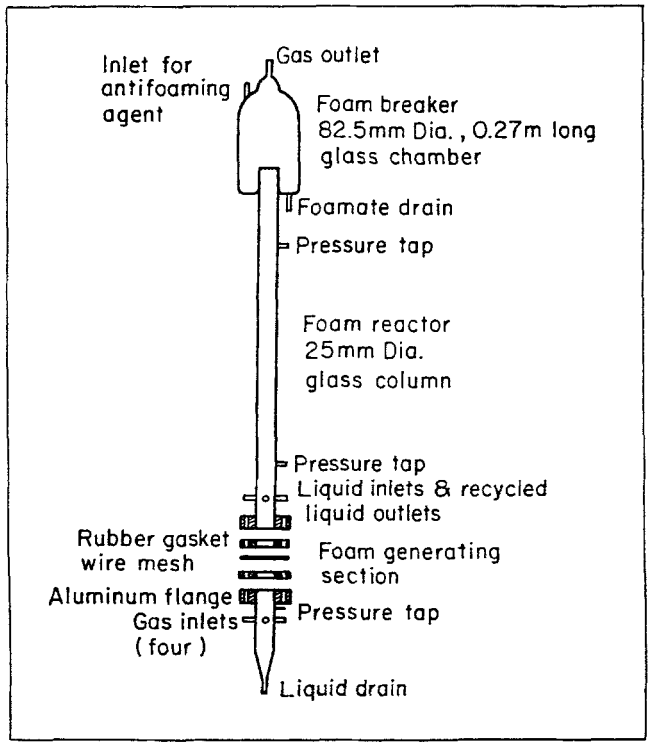

Figure 1. Foam reactor.

absorption of CO_2 into an aqueous slurry of small $Ca(OH)_2$ particles. The overall process of the carbonation of lime consists of the following steps:

$$Ca(OH)_2[s] \rightleftharpoons Ca^{2+} + 2OH^- \quad \text{(i)}$$

$$CO_2[g] \rightleftharpoons CO_2[aq] \quad \text{(ii)}$$

$$CO_2[aq] + OH^- \rightarrow HCO_3^- \quad \text{(iii)}$$

$$HCO_3^- + OH^- \rightarrow H_2O + CO_3^{2-} \quad \text{(iv)}$$

Reaction iv is instantaneous, and the rate-controlling steps could be the dissolution of $Ca(OH)_2$ and/or simultaneous absorption with chemical reaction of CO_2. When CO_2 is present along with a chemically-inert gas, some gas-side resistance for the transport of CO_2 from the bulk gas may also be important. The overall reaction may be written as:

$$CO_2 + 2OH^- \rightarrow CO_3^{2-} + H_2O \quad \text{(v)}$$

The absorption rate of CO_2 through the gas film may be given by:

$$(R_A|_{y=0})a_L = k_G a_L (p_A - p'_A) \quad (1)$$

For the situation when the mass transfer resistance associated with the dissolution of solids becomes important, that is, when:

$$\frac{k_s a_s C_{Bs}}{\nu} \cong \frac{a_L H p_A \sqrt{D_A k_2 C_{Bs} + k_L^2}}{\dfrac{1 + a_L H \sqrt{D_A k_2 C_{Bs} + k_L^2}}{k_G a_L}} \quad (2)$$

The absorption rate, according to Juvekar and Sharma (1973), is given by

$$(R_A|_{y=0})a_L = \frac{a_L C_{Ai} \sqrt{D_A k_2 C_{Bi} + k_L^2}}{\dfrac{1 + Ha_L \sqrt{D_A k_2 C_{Bi} + k_L^2}}{k_G a_L}} \quad (3)$$

In Eq. 3, the liquid-side concentration of reactant B at the gas-liquid interface is given by Juvekar and Sharma (1973):

$$C_{Bi} = C_{Bs} + Hp_A \sqrt{\frac{D_A}{D_B}} - (R_A|_{y=0})a_L \cdot \sqrt{\frac{HD_A}{k_G A_L D_B} + \frac{D_A}{k_L a_L D_B} + \frac{1}{k_s a_s}} \quad (4)$$

The solubility relationship at the gas-liquid interface is given by the Henry's law relationship:

$$C_{Ai} = Hp'_A \quad (5)$$

Combination of Eqs. 1, 3 and 5 gives:

$$(R_A|_{y=0})a_L = \frac{Ha_L p_A \sqrt{D_A k_2 C_{Bi} + k_L^2}}{\dfrac{1 + Ha_L \sqrt{D_A k_2 C_{Bi} + k_L^2}}{k_G a_L}} \quad (6)$$

When the gas-side resistance to solute mass transfer is negligible (large k_G) when compared with the liquid-side resistance or chemical reaction limitation, that is, when:

$$\frac{Ha_L \sqrt{D_A k_2 C_{Bi} + k_L^2}}{k_G a_L} \ll 1 \quad \text{and} \quad p_A \cong p'_A \quad (7a)$$

then Eq. 6 becomes:

$$(R_A|_{y=0})a_L = Ha_L p_A \sqrt{D_A k_2 C_{Bi} + k_L^2} \quad (7b)$$

Further, for

$$(D_A k_2 C_{Bi}) \gg k_L^2 \quad (8a)$$

Equation 7 becomes:

$$(R_A|_{y=0})a_L \cong Ha_L p_A \sqrt{D_A k_2 C_{Bi}} \quad (8b)$$

Elimination of the interfacial concentration of reactant B, C_{Bi}, from Eq. 8 may be accomplished in the following manner. From Eq. 3, consider the case when solids dissolution is the rate-limiting step. Then:

$$\frac{1}{k_s a_s} \gg \frac{H}{k_G a_L} \sqrt{\frac{D_A}{D_B}} \quad (9a)$$

and

$$\frac{1}{k_s a_s} \gg \frac{1}{k_L a_L} \sqrt{\frac{D_A}{D_B}} \quad (9b)$$

that is, when the gas- and liquid-side resistances may be neglected, Eq. 2 becomes:

$$C_{Bi} \cong C_{Bs} + Hp_A \sqrt{\frac{D_A}{D_B}} - (R_A|_{y=0})a_L \left(\frac{1}{k_s a_s}\right) \quad (9c)$$

Solution of Eq. 9 for $(R_A|_{y=0})a_L$ gives:

$$(R_A|_{y=0})a_L = C_{Bs} - C_{Bi} + Hp_A \sqrt{\frac{D_A}{D_B}} (k_s a_s) \quad (10)$$

$$C_{Bi} + \left[\frac{Ha_L p_A D_A k_2}{k_s a_s}\right] \sqrt{C_{Bi}} - \left[C_{Bs} + Hp_A \frac{D_A}{D_B}\right] = 0 \quad (11)$$

which is quadratic in $(C_{Bi})^{1/2}$.

Note that in Eq. 11,

(a) $C_{Bi} = C_{Bi}(p_A)$

(b) Only the positive root from Eq. 11 is meaningful. Therefore, Eq. 8, with Eq. 11, gives the expression for the absorption rate of CO_2 in the foam slurry reactor in the stable foam stage.

Additional transport properties

The partial pressure of reactant A in the gas stream is given by:

$$p_A = y_A P_T \quad (12)$$

Due to a pressure gradient in the axial direction, P_T is a function of z, given by:

$$P_T = P_{out} + \alpha(z - h_f) \tag{13}$$

From Danckwerts and Sharma (1966), the second-order rate constant for the reaction between CO_2 and OH^- at infinite dilution is given by:

$$\log_{10}(k_2) = 13.635 - \frac{2{,}895}{T} \tag{14}$$

where T is in K. In *their* Figure 6, k_2 is given as a function of ionic strength, I. In the present system, however, the solubility of $Ca(OH)_2$ is quite low and the surfactant concentration is also very low so that the value of k_2 at infinite dilution may be employed in all calculations.

For pure water, Haq (1982) gives the expression for the Henry's coefficient as:

$$\log_{10}(H^o) = 6.123 - (5.9044 \times 10^{-2})T + (7.885 \times 10^{-5})T^2 \tag{15}$$

where T is measured in K. For solubility of CO_2 in electrolyte solution. Onda et al. (1970) give the expression:

$$\log_{10}\frac{H}{H^o} = -kI \tag{16}$$

$$k = x_g + x_c + x_a \tag{17}$$

where x_g, x_c, and x_a are tabulated by Onda et al. (1970), and

$$I = \frac{z_c^2 C_c + z_a^2 C_a}{2} \tag{18}$$

According to Haq (1982), the diffusivity of CO_2 in pure water is given by:

$$\log_{10}(D_o) = -4.1764 + \frac{712.5}{T} - \frac{2.59 \times 10^5}{T^2} \tag{19}$$

Since $Ca(OH)_2$ is sparingly soluble and since data are not available to correct D_o for electrolyte concentration, Eq. 19 is the expression used to calculate D_A (i.e., $D_o = D_A$). The error is expected to be <1% (see, e.g., Hikita et al., 1976; Noulty and Leaist, 1984).

The gas-liquid interfacial area is given by:

$$a_L = \frac{6\epsilon_G}{d_s} \tag{20}$$

where the Sauter mean bubble diameter, d_s, is given by:

$$d_s = \frac{\sum_{j=1}^{n} N_j (d_{bj})^3}{\sum_{j=1}^{n} N_j (d_{bj})^2} \tag{21}$$

The solid-liquid interfacial area, a_s, is given by:

$$a_s = \frac{6w}{\rho_s d_p} \tag{22}$$

From the International Critical Tables (1928), the aqueous solubility of calcium hydroxide, C_{Bs}, is 4.36×10^{-2} kmol/m^3.

The overall absorption rate, R_A, is given by:

$$R_A = \frac{\int_0^{h_f} (R_A|_{y=0})\, dz}{\int_0^{h_f} dz} \tag{23}$$

Computational procedure

For plug flow of foam in the column's axial direction, a material balance on gas solute A gives:

$$\frac{-d\dot{n}_A}{dz} - (R_A|_{y=0}) a_L A_x = 0 \tag{24}$$

For a column of circular cross-section,

$$\Delta V = A_x \Delta z$$

and for ideal gases and an ideal gas mixture

$$\dot{n}_A = \frac{\dot{V}_G}{RT} p_A$$

Then Eq. 24 becomes:

$$\frac{dp_A}{dz} = \frac{-RT}{\dot{V}_G} a_L A_x (R_A|_{y=0}) \tag{25}$$

Equation 25, when used in conjunction with Eqs. 8, 11, 12 and 13, allows calculation of gas-phase solute concentration as a function of axial position in the stable foam stage of a three-phase foam-slurry reactor. The material balance relationship (Eq. 25) is expressed in terms of experimental parameters of liquid interfacial area, as well as the calculated quantity of absorption rate. These equations are integrated from the top of the liquid pool to the end of the stable foam stage. The result is that k_s, the solid-liquid mass transfer coefficient, may thus be determined semitheoretically for the stable foam section in the three-phase foam-slurry reactor.

Numerical integration of pertinent equations for the stable foam stage was performed with a fourth-order Runge Kutta integration technique. Essential elements of the algorithm are:

1. Definition of experimental conditions (T, P_{out}, etc.)
2. Calculation of quantities defined by experimental conditions
3. Calculation of the mass transfer rate, yielding gas-phase solute concentration as a function of position.

Since the solid-liquid mass transfer coefficient, k_s, was not known, it was determined iteratively, as a two-point boundary-value problem.

Experimental Studies

The three-phase foam slurry reactor is depicted schematically in Figure 1. The stable foam section was a vertical glass column of 0.025 m ID. Two foam reactors were used, differing only in the length of the stable foam section: 0.86 m and 0.41 m, respectively. A schematic representation of the complete experimental setup is shown in Figure 2.

The absorption, dissolution and reaction steps involved in the carbon dioxide-calcium hydroxide system were discussed previously in the Model Development section. Experimental conditions were chosen so as to meet the following criteria: (a) stable plug-flow of foam in the foam reactor, and (b) Eq. 4 is satisfied. The first criterion was required to allow for a quantitative description of a three-phase foam flow behavior, while the second allowed study of the system in the solids-dissolution rate-limiting regime. Note that the applicability conditions for Eqs. 1–13, as given by Eqs. 2, 7a, 8a, 9a and 9b, require various thermodynamic and transport parameters. The sources of these values are as follows: H, D_A, k_2, and C_{Bi} are taken from the literature, as noted in Eq. 14–18; k_G and k_L are from Shah and Mahalingam (1984); the rest were determined experimentally in this work. Substitution of these values into Eqs. 2, 7a, 8a, 9a and 9b validate the use of Eqs. 1–13 in this work.

From the theoretical model developed above, it is apparent that significant parameters in the operation of a three-phase foam slurry reactor are: solids loading, gas-liquid interfacial area, and foam flow rate.

First, a series of experimental runs were made with zero solids loading in order to determine the rate of gas solute absorption without chemical reaction. Next, in order to verify the theoretical model developed above, for the stable foam section of the foam reactor, experimental runs were made for three values of solids holdup in a 0.86-m-long reactor. In order to further validate the results of the computer simulations, another series of experimental runs were made in a 0.41-m-long reactor. All three series of runs involved CO_2 absorption in foam containing sodium dodecyl sulfate (SDS, 1.5% by weight, an anionic surfactant) at four different gas flow rates. The second series included three values of solids loading and three wire mesh sizes, while the third series involved three values of solids loading and only one mesh size. The inlet gas stream contained 10% CO_2 in air, and the particle sizes ranged from 2 to 6 μm. Further, in order to determine the effect of surfactant type on foam stability and reactor performance, two additional surfactants (cationic and nonionic) were evaluated.

The gas stream at the inlet and outlet of the foam reactor was analyzed for carbon dioxide with a Perkin-Elmer Sigma 300 gas chromatograph (GC), using a Chromosorb 101 column and a thermal conductivity detector. The slurry stream at the inlet and outlet of the foam reactor was analyzed for solids loading and solid particle size. Solids loading (i.e., the weight of solids per unit volume of slurry) was determined by evaporation and weighing. A "blank" sample (i.e., a sample of the supernatant in the slurry reservoir, containing no solid particles) was also taken in order to determine the contribution of the surfactant to the dry weight of an experimental sample (Friberg and Osborne, 1984). Solid particle size distribution was determined by removing a small portion of the slurry sample and observing it under

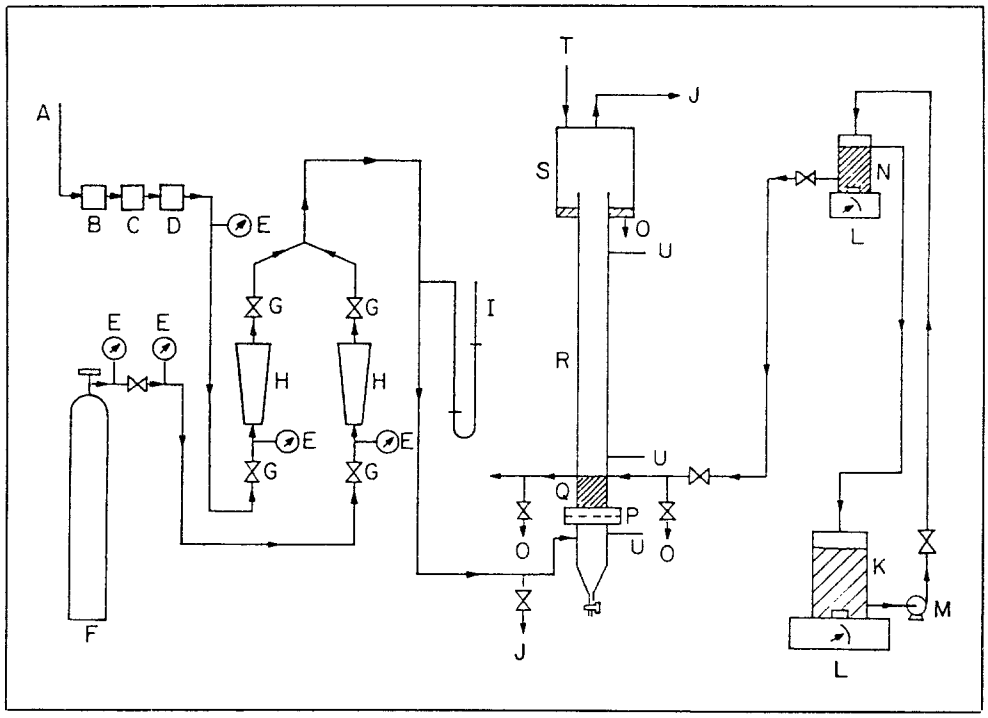

Figure 2. Experimental setup.

A = compressed air	H = flowmeter	O = slurry sampling port
B = filter	I = manometer	P = flange for wire mesh gas distributor
C = moisture removal column	J = gas sampling port	Q = foam generation section
D = pressure regulator	K = slurry reservoir	R = stable foam section
E = pressure gauge	L = magnetic stirring motor	S = foam disengagement section
F = CO_2 cylinder	M = pump	T = inlet for antifoaming agent
G = needle valve	N = constant-head tank	U = manometer ports

an Olympus BHM optical light microscope, with an Hitachi CCTV camera and video monitor, thus yielding the "Martin's diameter" for each solid particle (Allen, 1981). The foam bubble size distribution was determined by a photographic technique developed in this laboratory (Damle and Mahalingam, 1981), from which an average foam bubble size for each wire mesh was calculated. This is given in Table 1.

Results and Discussion

0.86-m foam reactor

A semitheoretical determination of the solid-liquid mass transfer coefficient was made for each of the experimental runs in the 0.86-m reactor. Typical results are shown in Figure 3. It may be seen that k_s decreases with increasing solids loading and increases with increasing gas flow rate and increasing wire mesh number (or decreasing foam bubble size). These are considerably lower figures for the solid-liquid mass transfer coefficient than those in alternative reactor configurations (see, e.g., Ramachandran and Sharma, 1969; Charpentier, 1982), which is to be expected in view of the higher degree of solids agitation inherent in conventional reactor configurations.

In order to understand the source of the difference in k_s values between those in the three-phase foam slurry reactor and those in alternative reactor configurations, it is necessary to consider the following points. First, it is instructive to compare the value of k_s for a solid particle in a conventional reactor (e.g., CSTR for which the range of k_s is typically 2×10^{-6} to 8×10^{-6} m/s) with that for the same particle suspended in a stagnant fluid medium. Since the liquid in the foam lamella, in which the particle is suspended, would be expected to flow past the particle with very low Reynolds number as based on particle diameter, this stagnant-fluid approximation (i.e., mass transfer in the absence of convection) might yield a reasonable first approximation to the true value of k_s. As the Reynolds number approaches zero, the Sherwood number (N_{Sh}) would assume a value of 2.0 (Marrone and Kirwan, 1986; Skelland, 1974). Since the Sherwood number is given by $N_{Sh} = k_s d_p / D_B$, a limiting value of k_s for a particle of 2×10^{-6} mm is $2D_B/d_p \cong 1 \times 10^{-3}$ m/s. However, since the k_s values determined here are roughly four orders of magnitude smaller than this, a second interpretation is required.

Dippenaar (1982) and Hemmings (1981) both describe the adsorption of surfactants on the surfaces of solid particles as necessary to ensure the success of a froth flotation process. The presence of a surfactant layer at the gas-liquid interface has been shown to add a significant resistance to interphase mass transfer (see, e.g., Davies and Rideal, 1961; Nguyen Ly et al., 1979; Springer and Pigford, 1970). Now, Shah and Mahalingam (1984) estimated that the CO_2 (solute) diffusivity through a thin surfactant layer may be as much as four orders of magnitude lower than that in the bulk liquid. A charged species such as OH^- in this case might be expected to possess even less mobility than a neutral molecule such as CO_2. The large difference in

Table 1. Relationship between Average Bubble Size and Mesh Size

Mesh Size	Avg. Bubble Size (m)
60	0.0014
100	0.0016
200	0.0020

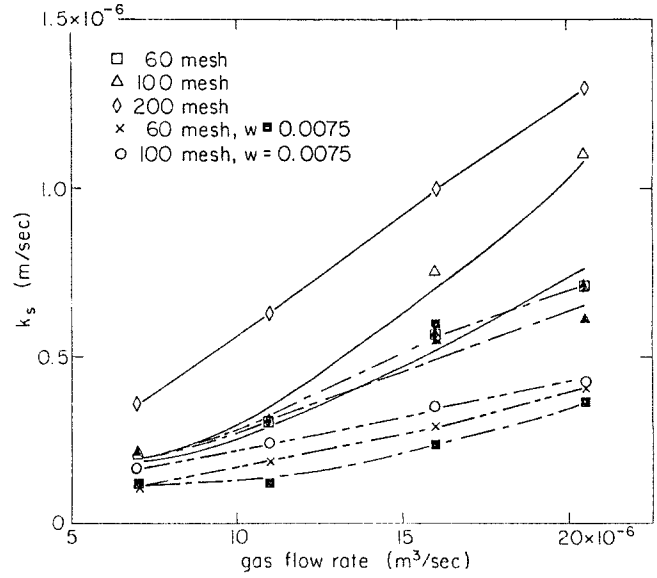

Figure 3. Solid-liquid mass transfer coefficient for a variety of operating conditions.
Filled symbol, $w = 0.0025$; open, $w = 0.0050$

k_s values shown in Table 2 might thus be explained by interfacial resistance to mass transfer due to the presence of a surfactant layer at the liquid-solid interface.

Alternately, low k_s values may be explained by invoking mechanisms other than mass transfer inhibition due to surfactant.

1. For example, low values of k_s might be due to slow kinetics of a chemical reaction taking place at the liquid-solid interface. The work of Chan and Rochelle (1982) and Sada et al. (1981), however, report extremely low values for k_s in an analogous gas-liquid-solid system, in which interfacial reactions are not occurring.

2. The film thickness of a bubble suggests that the thickness of the gas-liquid and solid-liquid mass transfer films, as well as that of the soap film itself, would each be of comparable magnitude. As a result, k_s should be higher for a thin liquid film of finite thickness than for a semiinfinite medium; however, because of the presence of surfactant, the k_s values are lower. Sada et al. (1981) have shown indeed that the presence of very fine particles near the gas-liquid interface would actually lead to the enhancement of gas absorption; however, their work does not include surfactants.

3. The possibility of mass transfer limitation, due to the retarded diffusion of calcium ions in the bubble film, does not appear to be a likely explanation. Much of the $Ca(OH)_2$ particles reside in and dissolve into the bubble film. Most of the CO_2

Table 2. Transport Parameters for Various Reactor Configurations

Reactor Type	Gas Holdup	$a_L(10^3\ m^2/m^3)$	$k_s(10^{-6}$ m/s)
Foam Column*	>0.9	24–39	0.02–0.3
Bubble Column**	<0.5	1–18	2–8
CSTR**	<0.3	1–6	2–8

*This work.
**See, e.g., Juvekar and Sharma (1973).

is also absorbed into the bubble film. Thus, the chemical reaction would take place in the bubble film. The net transport of calcium ions would take place more by convective transport than by diffusion, the former which takes place due to film drainage and thinning which transport the water and the calcium ions to the Plateau borders of the foam. The low values of k_s are thus likely explained by the mass transfer resistance due to the presence of surfactant at the solid-liquid interface.

Foam stability enhancement was expected to be improved by the presence of solid particles in the foam (Bikerman, 1973; Dippenaar, 1982; Hemmings, 1981; Thonavadi and Lemlich, 1983). Enhancement of foam stability was not, however, observed visually in this series of experimental runs. This was apparently due to the fact that the average particle sizes of 4×10^{-6} m was smaller than the optimum size for promotion of foam stability ($3–4 \times 10^{-5}$ m) (Thonavadi and Lemlich, 1983). Foam instability was most pronounced at higher gas flow rates, when the onset of flow channeling was observed in the foam reactor. Further, it was not possible to generate stable foams for conditions of $w = 0.0075$ kg/kg and the finer 200-mesh screen size, which was also probably due, in part, to some fouling of the wire mesh screen.

Gas-liquid interfacial area, a_L, depends upon gas holdup and Sauter mean foam bubble diameter (Eq. 21). Graphical representation of a_L vs. gas flow rate for various solids loading is given in Figure 4. As expected from previous work in this laboratory (Damle, 1980; Shah, 1983; Shah and Mahalingam, 1984), gas-liquid interfacial area depended almost exclusively upon wire mesh screen size, and negligibly upon gas flow rate and solids loading for the ranges examined experimentally. Since foam bubble size is determined by orifice size in the gas distribution plate (Kumar and Kuloor, 1970), a strong dependence of foam bubble size on wire mesh screen size is to expected. Further, since foam bubble size does not depend much upon gas flow rate and since gas holdup depends only slightly on gas flow rate, the gas-liquid interfacial area in the stable foam section, as calculated by Eq. 20, should not depend much upon gas flow rate. Finally, solids loading did not significantly affect gas-liquid interfacial area, probably due to the fact that the solids loadings

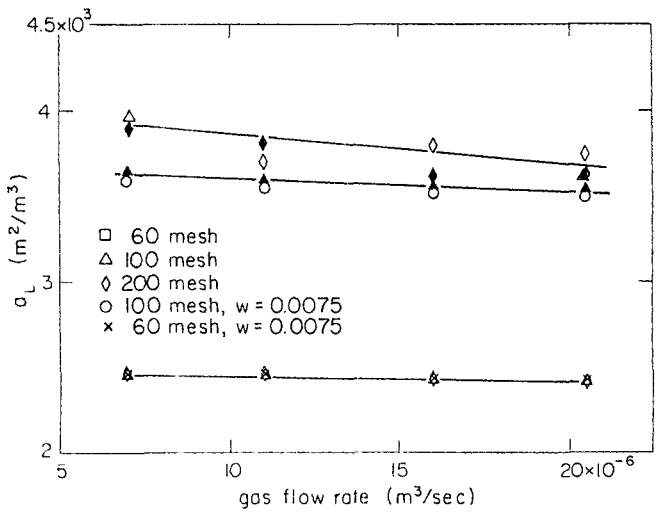

Figure 4. Gas-liquid interfacial area in stable foam section for a variety of operating conditions.
Filled symbol, $w = 0.0025$; open, $w = 0.0050$

which permitted a stable three-phase foam to be generated were relatively small.

Solid-liquid interfacial area, a_s, depends upon solids loading, particle size, and particle density (Eq. 22). Because calcium hydroxide was the only solid phase involved, the particle density remained fixed; the particle size was also constant, since all calcium hydroxide required for the experimental work came from the same lot. Thus, solid-liquid interfacial area was adjusted only through changing solids loading, to which a_s was directly proportional. By varying solids loading over a threefold range of values, it was possible to study a range of solid-liquid interfacial areas from 3.1×10^3 to 9.3×10^3 m^2 per m^3 of liquid. Such a large interfacial area was possible in a three-phase foam slurry reactor because the amount of liquid contained in the foam was relatively small.

0.41-m foam reactor

In order to validate the results of the computer simulation runs, a series of experimental runs was made in a 0.41-m-long foam reactor. This foam reactor was fabricated in such a way that all portions of the reactor were nearly identical to that of the 0.86-m foam reactor, except for the length of the stable foam section between pressure taps, which was 0.15 m for the former and 0.61 m for the latter. Experimental conditions were chosen to determine the effects of solids loading and gas flow rate. The effect of foam bubble size was not investigated since only one wire mesh sceen size (100 mesh) was employed and this parameter was studied in the series of runs with the 0.86-m foam reactor. The runs in the 0.41-m reactor allowed for evaluation of the solid-liquid mass transfer coefficient, average gas absorption rate, stability considerations, gas-liquid interfacial area, gas holdup, foam bubble size, solid-liquid interfacial area, and pressure drop across foam formation stable foam sections, and for comparison with analogous experimental runs in the 0.86-m foam reactor. The results for k_s and stability enhancements are discussed below.

The solid-liquid mass transfer coefficient, k_s, was determined semitheoretically with the use of a differential-equation-solving software package for each of the experimental runs in the 0.41-m foam reactor. The results are presented graphically in Figure 5. It may be seen from this figure that k_s increased with decreasing solids loading and increasing gas flow rate. The values of the solid-liquid mass transfer coefficient for the 0.41-m foam reactor corresponded with those in the 0.86-m foam reactor, as shown in Figure 6. The small differences were undoubtedly due to entrance effects in the stable foam section, which would be more pronounced in the half-height (0.41-m) reactor, since the liquid holdup is known to be slightly higher at the beginning of the stable foam stage (Desai and Kumar, 1983). The liquid drainage occurring in this initial portion of the stable foam stage could lead to somewhat higher k_s values in this portion, whose effect would be to cause the (volume-averaged) solid-liquid mass transfer coefficient to appear greater in the 0.41-m foam reactor than that in the 0.86-m reactor. A possible resolution of this discrepancy would be to use the k_s value determined in the 0.41-m reactor for the first portion of the 0.86-m reactor and use a second value for k_s in the second portion of the larger reactor, thus accounting for the entrance effects in both reactors.

Foam stability enhancement, due to particulate loading, was not observed to be improved in the 0.41-m foam reactor, when compared with that in the 0.86-m foam reactor, as to be

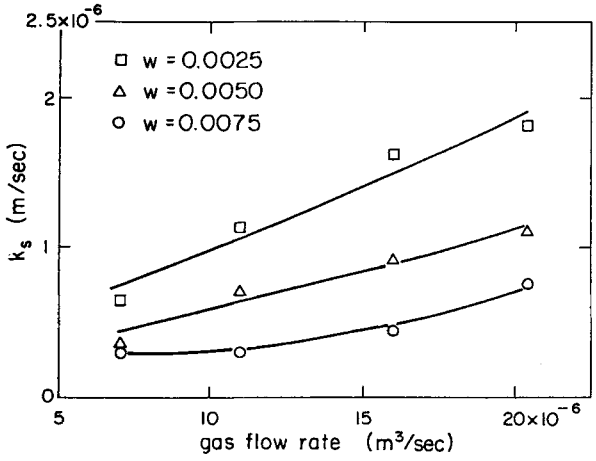

Figure 5. Solid-liquid mass transfer coefficient in 0.41-m reactor (100 mesh).

expected. Foam instability, again, was most pronounced at higher gas flow rates, when the onset of flow channeling was observed in the foam reactor. The same experimental difficulties in generating a stable three-phase foam flowing in the plug-flow regime were experienced in the 0.41-m reactor runs, for solids loadings greater than 0.075 kg/kg and gas flow rates greater than 2.0×10^5 m^3/s, as was the case in the 0.86-m foam reactor.

Comparison with conventional reactor configurations

In order to demonstrate the advantages of employing this novel gas-liquid-solid contacting device, it is important to compare the relevant transport parameters of this three-phase foam slurry reactor with those of more conventional chemical reactor configurations. The transport parameters of gas holdup, gas-liquid interfacial area and solid-liquid mass transfer coefficient for the foam column reactor, bubble column reactor and CSTR are given in Table 2. For additional comparisons, see also Charpentier (1982).

It may be seen in Table 2 that gas holdup is much greater in a foam column reactor than in other reactor configurations. This is advantageous in the situation where large quantities of gas are to be treated with a relatively small amount of slurry. It is also

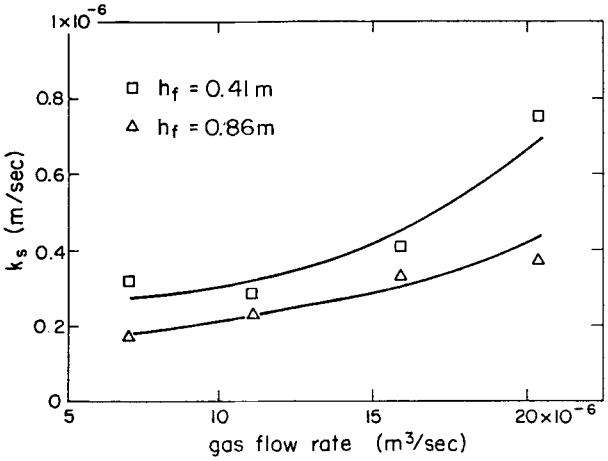

Figure 6. Comparison of k_s values between 0.41-m and 0.86-m foam reactors.

apparent from Table 2 that it is possible to achieve a much larger gas-liquid interfacial area in a foam reactor, as compared with, e.g., stirred tank and bubble column reactors. This allows a much smaller reactor volume to be used when a specified total gas-liquid interfacial area is required. Finally, a disadvantage of the foam reactor is seen in Table 2, where it is apparent that the solid-liquid mass transfer coefficient is much lower in a foam reactor than in either of the other reactor configurations; this is probably due to the much higher degree of solids agitation possible in the bubble column and CSTR than in the foam reactor. This disadvantage is offset, however, by the larger a_L and ϵ_G values in the foam column, and also by average absorption rates in a foam reactor, based upon unit volume of reactor that are comparable to those in these two alternative reactor configurations (see, e.g., Capuder and Koloini, 1984; Juvekar and Sharma, 1973; Ramachandran and Sharma, 1969). Thus, under certain limited conditions, the three-phase foam slurry reactor could perform superior to other chemical reactor configurations.

Acknowledgment

The experimental and theoretical work was supported by a Standard Oil Fellowship for one of the authors (G.C.S.) and by Washington State University. Preparation of the manuscript was supported by the Advanced Materials Technology Program, Washington Technology Center, University of Washington, under Grants AFOSR-83-0375 and AFOSR-87-0114.

Notation

a_L = gas-liquid interfacial area, m^2/m^3 reactor volume
a_s = solid-liquid interfacial area, m^2/m^3 liquid
A_x = column cross-sectional area, m^2
C_a = anion concentration, Eq. 18, kmol/m^3
C_{Ai} = liquid-side concentration of A at gas-liquid interface, kmol/m^3
C_{Bi} = liquid-side concentration of B at gas-liquid interface, kmol/m^3
C_{Bs} = saturation concentration of OH^- ions (B) in aqueous solution in equilibrium with $Ca(OH)_2$[s], kmol/m^3
C_c = cation concentration, Eq. 18, kmol/m^3
d_s = Sauter mean bubble diameter, m
D_A = liquid-phase diffusivity of A, m^2/s
D_B = liquid-phase diffusivity of B, m^2/s
d_{bj} = diameter of jth foam bubble, m
D_o = diffusivity of A in pure water, m^2/s
d_p = particle diameter, m
h_f = height of stable foam section, m
H = Henry's coefficient for CO_2 in electrolyte solution, kmol/m^2 · Pa
H^o = Henry's coefficient for CO_2 in pure water, kmol/m^2 · Pa
I = ionic strength, kmol/m^3
k = salting-out parameter, Eq. 16, kmol/m^3
k_2 = second-order reaction rate constant between CO_2 and OH^-, m^3/kmol · s
k_G = gas-side mass transfer coefficient, kmol/Pa · m^2 · s
k_L = liquid-side mass transfer coefficient, m/s
k_s = solid-liquid mass transfer coefficient, m/s
$\dot{n}_A$ = molar flow rate of A in gas phase, m/s
N_{bj} = number of bubbles having diameter, d_{bj}
p_A = bulk gas partial pressure of A, Pa
p'_A = gas-side partial pressure of A at gas-liquid interface, Pa
P_{out} = ambient pressure at column outlet, Pa
R = gas constant, m^3 · Pa · kmol · K
$\overline{R}_A$ = average absorption rate of A, kmol/m^2 · s
V = reactor volume, m^3
V_G = total volumetric gas flow rate, m^3/s
w = solids loading, kg/m^3
x_a, x_c, x_g = defined by Eq. 17, m^3/kmol
y = distance normal to gas-liquid interface, m
y_A = mole fraction of solute A in gas phase
z = axial position coordinate, m

z_a = charge on anion, Eq. 18
z_c = charge on cation, Eq. 18

Greek letters

α = pressure gradient in stable foam section, Pa/m
ϵ_G = gas holdup in stable foam section
ν = stoichiometric coefficient for the reaction $A + \nu B \rightarrow$ products
ρ_s = particle density, kg/m^3

Literature Cited

Allen, T., *Particle Size Measurement*, 3rd ed., Chapman and Hall, New York (1981).

Asolekar, S. R., P. K. Deshpande, and R. Kumar, "A Model for a Foam-Bed Slurry Reactor," *AIChE J.*, **34**, 150 (1988).

Bhaskarwar, A. N., and R. Kumar, "Oxidation of Sodium Sulfate in a Foam Bed Contactor," *Chem. Eng. Sci.*, **39**, 1393 (1984).

———, "Oxidation of Sodium Sulphide in the Presence of Fine Activated Carbon Particles in a Foam Bed Contactor," *Chem. Eng. Sci.*, **41**, 399 (1986).

———, "Mass Transfer Accompanied by a Chemical Reaction in an Emulsion Foam Bed Reactor," *AIChE J.*, **33**, 331 (1987).

Bikerman, J. J., *Foams*, Springer-Verlag, New York (1973).

Biswas, J., and R. Kumar, "Mass Transfer with Chemical Reaction in a Foam Bed Contactor," *Chem. Eng. Sci.*, **36**, 1547 (1981).

Brander, S. M., G. I. Johansson, B. G. Kronberg, and P. J. Stenins, "Reactive Foams for Air Purification," Int. Cong. in Scandinavia on Chemical Engineering, Copenhagen (1983).

Capuder, E., and T. Koloini, "Gas Holdup and Interfacial Area in Aerated Suspensions of Small Particles," *Chem. Eng. Res. Dev.*, **62**, 255 (1984).

Chan, P. K., and T. Rochelle, "Limestone Dissolution: Effects of pH, CO_2, and Buffers Modeled by Mass Transfer," *ACS Symp. Ser.*, **188**, 75 (1982).

Charpentier, J. C., "What's New in Absorption with Chemical Reactions?," *Trans. Inst. Chem. Eng.*, **60**, 131 (1982).

Cheng, H. C., and R. Lemlich, "Errors in the Measurement of Bubble Size Distribution in Foam," *Inst. and E. C. Fund.*, **22**, 105 (1983).

Damle, A. S., "Gas-Submicron Particles Separation in a Flowing Liquid Foam Bubble Matrix," PhD Thesis, Washington State Univ., Pullman, WA (1980).

Damle, A. S., and R. Mahalingam, "Behavior of Polydisperse Aerosols Inside a Closed Sphere," *J. Colloid Interf. Sci.*, **87**, 242 (1982).

Danckwerts, P. V., and M. M. Sharma, "The Absorption of Carbon Dioxide into Solutions of Alkalis and Amines (with some notes on hydrogen sulphide and carbonyl sulphide)," Review Series No. 2, *The Chem. Eng.*, CE244-CE280 (Oct., 1966).

Davies, J. T., and E. K. Rideal, *Interfacial Phenomena*, Academic Press, New York (1961).

Desai, D., and R. Kumar, "Liquid Holdup in Semi-Batch Cellular Foams," *Chem. Eng. Sci.*, **38**, 1525 (1983).

Dippenaar, A., "The Destabilization of Froth by Solids. I. The Mechanism of Film Rupture," *Int. J. of Mineral Process.*, **9**, 1 (1982).

Friberg, S. E., and D. W. Osborne, "Solubilization of Calcium Dodecyl Sulphate in a Micellular Solution and in Lamellar Liquid Crystal," *Colloids and Surfaces*, **12**, 357 (1984).

Froment, G. F., and K. B. Bischoff, *Chemical Reactor Analysis and Design*, Wiley, New York (1979).

Haq, M. A., "Fluid Dynamics on Sieve Trays," *Hydroc. Process.*, 165 (Apr., 1982).

Hemmings, C. E., "On the Significance of Flotation Froth Liquid Lamella Thickness," *Trans. Instn. Min. Metall.* (Sect. C: Mineral Process. Extr. Metall.), 90 C96–C102 (1981).

Hikita, H., S. Asai, and T. Takatsaka, "Absorption of Carbon Dioxide into Aqueous Sodium Hydroxide and Sodium Carbonate-Bicarbonate Solutions," *Chem. Eng. J.*, **11**, 131 (1976).

Juvekar, V. A., and M. M. Sharma, "Absorption of CO_2 in a Suspension of Lime," *Chem. Eng. Sci.*, **28**, 825 (1973).

Kumar, R., and N. R. Kuloor, "The Formation of Bubbles and Drops," *Adv. Chem. Eng.*, **8**, 256 (1970).

Lemlich, R., "Morphology and Interbubble Gas Diffusion in Foam," AIChE Meeting, Washington, DC (Oct. 30–Nov. 4, 1983).

Limaye, R. S., "Studies Involving Foam, Submicron Particles and Laser Doppler Anemometry," MS Thesis, Washington State Univ. (1976).

Lutsko, F. N., A. T. Bartov, A. P. Prokopenko, and E. A. Orlov, "Two-Phase Model of Absorption in a Foam Layer," cited in *Chem. Abst.*, **95**, 205994k (1981).

Mahalingam, R., H. S. Surati, and J. A. Brink, Jr., "High-Expansion Foam Flow Analyses," *AIChE Symp. Ser.*, **150**(70), 52 (1975).

Mahalingam, R., and J. A. Brink, Jr., "High-Expansion Liquid Foams in Submicron Particle Emission Control," Tech. Report to Electric Power Research Institute, Palo Alto, CA (1978).

Maminov, O. V., and A. Mutriskov, "Mass Transfer Behavior in Foam Layers," *Int. Chem. Eng.*, **9**, 642 (1969).

Marrone, G. M., and D. J. Kirwan, "Mass Transfer to Suspended Particles in Gas-Liquid Agitated Systems," *AIChE J.*, **32**, 523 (1986).

Metzner, A. B., and L. F. Brown, "Mass Transfer in Foams," *Ind. Eng. Chem.*, **46**, 2040 (1956).

Nguyen Ly, L. A., R. G. Carbonell, and B. J. McCoy, "Diffusion of Gases Through Surfactant Films: Interfacial Resistance to Mass Transfer," *AIChE J.*, **25**, 1015 (1979).

Noulty, R. A., and D. G. Leaist, "Activity Coefficients and Diffusion Coefficients of Dilute Aqueous Solutions of Lithium, Sodium, and Potassium Hydroxides," *J. Solution Chemistry*, **13**, 767 (1984).

Onda, K., E. Sada, T. Kobayashi, S. Kito, and K. Ito, "Salting-Out Parameters of Gas Solubility in Aqueous Salt Solutions," *J. Chem. Eng. Japan*, **3**, 18 (1970).

Pasiuk-Bronikowska, W., and A. Sokolowski, "Activation Energy Variations for Catalytic Oxidations of Aqueous SO_2," *Chem. Eng. Sci.*, **38**, 121 (1983).

Ralston, J., "Thin Films and Froth Flotation," *Adv. in Colloid and Interf. Sci.*, **19**, 1 (1983).

Ramachandran, P. A., and R. V. Chaudhari, *Three-Phase Catalytic Reactors*, Gordon and Breach, New York (1983).

Ramachandran, P. A., and M. M. Sharma, "Absorption with Fast Reacton in a Slurry Containing Sparingly Soluble Fine Particles," *Chem. Eng. Sci.*, **24**, 1681 (1969).

Sada, E., H. Kumazawa, Y. Sawada, and I. Hashizume, "Kinetics of Absorptions of Lean Sulfur Dioxide into Aqueous Slurries of Calcium Carbonate and Magnesium Hydroxide," *Chem. Eng. Sci.*, **36**, 149 (1981).

Schlichting, H., *Boundary-Layer Theory*, McGraw-Hill, New York (1979).

Shah, P. S., "Mass Transfer with Chemical Reaction in Liquid Foam Reactors," MS Thesis, Washington State Univ. (1983).

Shah, P. S., and R. Mahalingam, "Mass Transfer with Chemical Reaction in Liquid Foam Reactors," AIChE Meeting, Denver (Aug. 28–31, 1983).

———, "Mass Transfer with Chemical Reaction in Liquid Foam Reactors," *AIChE J.*, **30**, 924 (1984).

Shah, Y. T., *Gas-Liquid-Solid Reactor Design*, McGraw-Hill, New York (1978).

Skelland, A. H. P., *Diffusional Mass Transfer*, Wiley, New York (1978).

Springer, T. K., and R. L. Pigford, "Influence of Surface Turbulence and Surfactants on Gas Transport Through Liquid Interfaces," *Int. and EC Fund.*, **9**, 458 (1970).

Stangle, G. C., "Mass Transfer with Chemical Reaction in a Three-Phase Foam-Slurry Reactor," PhD Thesis, Washington State Univ. (1985).

Stangle, G. C., and R. Mahalingam, "Mass Transfer with Chemical Reaction During Gas Bubble Formation in Foam Column Reactors," *Chem. Eng. Sci.*, **44**, 507 (1989).

Surati, H. S., "Submicron Particulate Collection in a Foam Column," MS Thesis, Washington State Univ. (1975).

Tadaki, T., and S. Maeda, "Absorption of Carbon Dioxide by Milk of Lime in a Wetted-Wall Column," *Kagaka Kogaka*, **2**, 85 (1964).

Thonavadi, N. N., and R. Lemlich, "Flow Properties of Foam With and Without Solid Particulates," AIChE Meeting, Washington, DC (Nov., 1983).

Washburn, E. W., *International Critical Tables*, McGraw-Hill, New York (1928).

Wilson, D. J., "Adsorbing Colloid Flotation Methods," *Theory, Practice and Process Principles for Physical Separations*, M. P. Freeman and J. A. FitzPatrick, eds., Engineering Foundation, New York (1981).

Manuscript received July 2, 1987, and revision received Oct. 10, 1989.